

The following resources related to this article are available online at www.sciencemag.org (this information is current as of August 17, 2009):

Updated information and services, including high-resolution figures, can be found in the online version of this article at:

<http://www.sciencemag.org/cgi/content/full/309/5735/755>

Supporting Online Material can be found at:

<http://www.sciencemag.org/cgi/content/full/309/5735/755/DC1>

This article **cites 24 articles**, 10 of which can be accessed for free:

<http://www.sciencemag.org/cgi/content/full/309/5735/755#otherarticles>

This article has been **cited by** 94 article(s) on the ISI Web of Science.

This article has been **cited by** 6 articles hosted by HighWire Press; see:

<http://www.sciencemag.org/cgi/content/full/309/5735/755#otherarticles>

This article appears in the following **subject collections**:

Chemistry

<http://www.sciencemag.org/cgi/collection/chemistry>

Information about obtaining **reprints** of this article or about obtaining **permission to reproduce this article** in whole or in part can be found at:

<http://www.sciencemag.org/about/permissions.dtl>

and in LSVCs), their fraction increases from 2.2% to 3.0%, similar to the increase in the fraction of single surface vacancies (from 1.5% to 3.0%). This indicates that the subsurface vacancies are essential for LSVc nucleation, which could occur via an intermediate surface–subsurface vacancy dimer (Fig. 4), the only vacancy dimer that has been observed (two occurrences in Fig. 1B, upper right).

Our observations show that electron localization determines which defects are formed on a ceria surface. The structural requirement of one subsurface vacancy per LSVc reveals the high propensity of Ce toward reduction upon O loss: Only Ce³⁺ ions are coordinated to the VC. Although this propensity favors further O release after double LSVcs have been formed, it may hamper their nucleation; the two electrons liberated by each of the first two missing O atoms are insufficient to reduce all of the coordinated Ce ions.

In real catalytic applications, one way to increase oxygen release from ceria while enhancing the thermal stability of its surface area and porosity (27) is by doping with Zr⁴⁺ ions, which are not reduced upon O loss (28). These two effects, increased oxygen release and thermal stability, seem irreconcilable but can be rationalized in light of our results: Preliminary calculations show that, with respect to the pure ceria (111) surface, the single vacancy formation around single Zr⁴⁺ dopants is facilitated

by 0.9 eV. Once formed, these vacancies can grow into VCs without further requiring the presence of subsurface vacancies and the related major structural rearrangement.

References and Notes

- G. A. Deluga, J. R. Salge, L. D. Schmidt, X. E. Verykios, *Science* **303**, 993 (2004).
- K. Otsuka, T. Ushiyama, I. Yamanaka, *Chem. Lett.* **9**, 1517 (1993).
- A. Trovarelli, Ed., *Catalysis by Ceria and Related Materials* (Imperial College Press, London, 2002).
- S. Park, J. M. Vohs, R. J. Gorte, *Nature* **404**, 265 (2000).
- S. Bernal *et al.*, *Catal. Today* **50**, 175 (1999).
- R. Schaub *et al.*, *Science* **299**, 377 (2003); published online 12 December 2002 (10.1126/science.1078962).
- E. Wahlström *et al.*, *Science* **303**, 511 (2004).
- C. T. Campbell, *Science* **299**, 357 (2003).
- M. D. Rasmussen, L. M. Molina, B. Hammer, *J. Chem. Phys.* **120**, 988 (2004).
- M. S. Chen, D. W. Goodman, *Science* **306**, 252 (2004); published online 26 August 2004 (10.1126/science.1102420).
- D. R. Mullins, S. H. Overbury, D. R. Huntley, *Surf. Sci.* **409**, 307 (1998).
- L. Wu *et al.*, *Phys. Rev. B* **69**, 125415 (2004).
- G. R. Rao *et al.*, *J. Catal.* **162**, 1 (1996).
- A. Martinez-Arias *et al.*, *J. Chem. Soc. Faraday Trans.* **91**, 1679 (1995).
- Q. Fu, H. Saltsburg, M. Flytzani-Stephanopoulos, *Science* **301**, 935 (2003); published online 3 July 2003 (10.1126/science.1085721).
- Z.-P. Liu, S. J. Jenkins, D. A. King, *Phys. Rev. Lett.* **94**, 196102 (2005).
- H. Nörenberg, G. A. D. Briggs, *Phys. Rev. Lett.* **79**, 4222 (1997).
- H. Nörenberg, G. A. D. Briggs, *Surf. Sci.* **424**, L352 (1999).
- K. Fukui, Y. Namai, Y. Iwasawa, *Appl. Surf. Sci.* **188**, 252 (2002).

- Y. Namai, K. Fukui, Y. Iwasawa, *Catal. Today* **85**, 79 (2003).
- Y. Namai, K. Fukui, Y. Iwasawa, *J. Phys. Chem. B* **107**, 11666 (2003).
- Strong correlation effects due to localization are modeled by adding a Hubbard-U term to the energy functional expressed in the pseudo-potential plane-wave framework. Details of the calculation can be found in (23, 24) and in the supporting online material.
- M. Cococcioni, S. de Gironcoli, *Phys. Rev. B* **71**, 035105 (2005).
- S. Fabris, S. de Gironcoli, S. Baroni, G. Vicario, G. Balducci, *Phys. Rev. B* **71**, 041102 (2005).
- Z. Yang, T. K. Woo, M. Baudin, K. Hermansson, *J. Chem. Phys.* **120**, 7741 (2004).
- Statistical evaluation of vacancy occurrences has an error margin of ±0.5% because of some ambiguous defect assignments (see “other” in Fig. 1).
- G. Colón *et al.*, *Catal. Today* **50**, 271 (1999).
- P. Fornasiero *et al.*, *J. Catal.* **164**, 173 (1996).
- We thank M. Gerunda and P. Facci for providing the STM tips, and S. Baroni, S. de Gironcoli, M. Graziani, and F. Rosei for fruitful discussions and critical reading of the manuscript. S.F. thanks Consorzio Interuniversitario CINECA for computing time. Supported by the International Centre for Theoretical Physics (ICTP) Training and Research in Italian Laboratories (TRIL) program (L.Z.), INSTM, Sincrotrone Trieste ScpA, and Ministero dell’Istruzione, dell’Università e della Ricerca (MIUR) under the programs FIRB 2001 (grant RBNE0155X7), COFINLAB 2001 (grant CLAB013P24), and COFIN 2003.

Supporting Online Material

www.sciencemag.org/cgi/content/full/309/5735/752/DC1

Materials and Methods

Fig. S1

References

28 February 2005; accepted 27 May 2005
10.1126/science.1111568

A Light-Actuated Nanovalve Derived from a Channel Protein

Armağan Koçer,^{1*} Martin Walko,^{2*} Wim Meijberg,^{1†}
Ben L. Feringa^{2†}

Toward the realization of nanoscale device control, we report a molecular valve embedded in a membrane that can be opened by illumination with long-wavelength ultraviolet (366 nanometers) light and then resealed by visible irradiation. The valve consists of a channel protein, the mechanosensitive channel of large conductance (MscL) from *Escherichia coli*, modified by attachment of synthetic compounds that undergo light-induced charge separation to reversibly open and close a 3-nanometer pore. The system is compatible with a classical encapsulation system, the liposome, and external photochemical control over transport through the channel is achieved.

Among addressable nanoscale devices, photo-induced molecular switches stand out for their ability to convert an optical input into a variety of useful output signals (1). Their short response times and reversibility allow switching

between different states rapidly and repeatedly. These molecular switches can be used to modulate the properties of materials at the bulk level, such as surface wettability (2), refractive index (3), or the lateral pressure profile of bilayers (4), as well as at the single-molecule level, for example, involving host-guest interactions (5) or the activity of enzymes (6). A particularly challenging and appealing application of photoswitches would be gating channels, thereby externally modulating ion flow and, by extension, drug release. Our approach has been to append an addressable photosensitive gate to a naturally occurring channel

protein, which ordinarily controls the exchange of solutes across the lipid bilayers that separate cells and organelles from their environment.

One of the best-characterized channel proteins is the mechanosensitive channel of large conductance, or MscL, from *Escherichia coli* (7). In nature, this protein functions as a safety valve to protect the bacterial cell against severe osmotic downshifts (8). A sudden influx of water results in the buildup of turgor pressure, generating tension in the membrane. Above a certain threshold value, the pressure results in the opening of a large, nonselective pore in the protein, about 3 nm in diameter (9), that allows efflux of ions, small solutes, and even some small proteins in an effort to prevent cell lysis (10, 11). Because of the large energetic cost that this process represents to the cell, the protein is tightly closed under normal conditions. Structural models of the protein and its gating mechanism have their basis in a large body of data from *E. coli* MscL and the crystal structure of its homolog from *Mycobacterium tuberculosis* (12–21). The protein is a homopentamer with two transmembrane helices, M1 and M2, per subunit. The actual pore of the channel is formed by five M1 helices. Although normally the channel opens in response to tension, the introduction of polar or charged amino acids (16) or other charged compounds (22) into the 22nd amino acid position of MscL leads to spontaneous opening of the channel; this charge effect also operates in

¹BiOMaDe Technology Foundation, Nijenborgh 4, 9747 AG Groningen, Netherlands. ²Department of Organic and Molecular Inorganic Chemistry, Stratingh Institute and Material Science Centre, University of Groningen, Nijenborgh 4, 9747 AG Groningen, Netherlands.

*These authors contributed equally to this work.

†To whom correspondence should be addressed. E-mail: B.L.Feringa@rug.nl (B.L.F.); meijberg@biomade.nl (W.M.)

other gated channels with closed hydrophobic pores (23).

In the case of MscL, hydrophilic substitutions into the narrow pore constriction area cause hydration of the pore and weakening of the hydrophobic van der Waals forces responsible for the close packing of the M1 helices in the closed

state of the channel. The effect is reinforced if charged or bulky groups are introduced because of electrostatic repulsion and steric factors, respectively. This is reflected in the energetics of the gating transitions, in particular the first subtransition from the closed to the first subconducting state, which is also the major energy

barrier for opening the wild-type channel. Within the framework of the “two gates model,” this transition represents the opening of the main gate, resulting in an expanded conformation with a low level of conductance attributed to blocking of the pore lumen by a second gate. Opening of this gate needs further energy input and leads to full con-

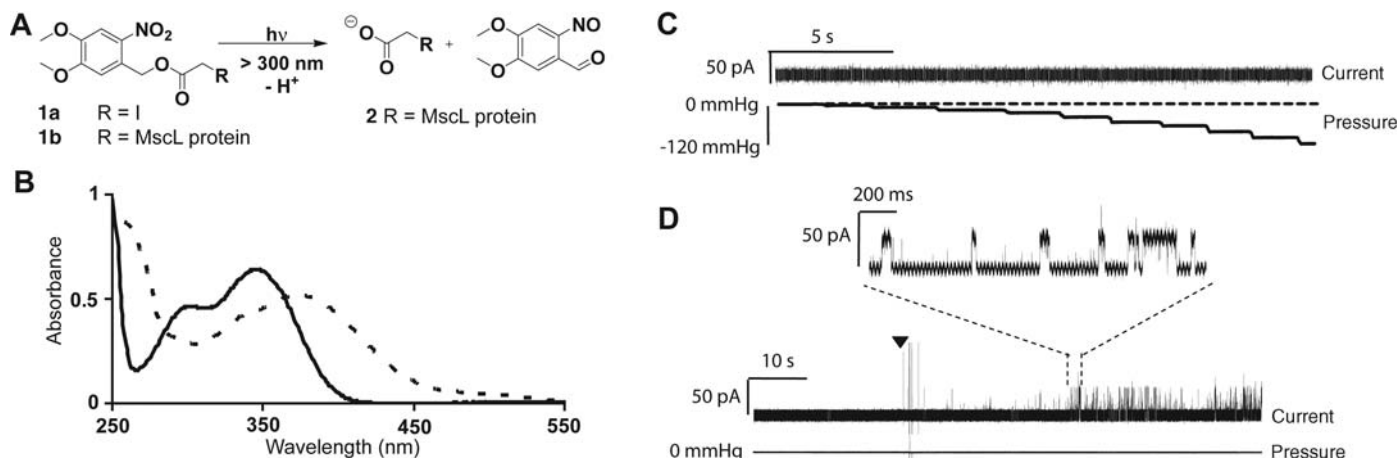


Fig. 1. A one-way photoswitch converts the MscL channel protein into a light-actuated valve. (A) Photolysis of compound 1 liberates charged acetate 2. (B) UV-visible spectrum of the solution of compound 1a before irradiation (full line) and after 5-min exposure to UV light (>300 nm) (dashed line). The disappearance of the absorption band at 346 nm and appearance of a band at 374 nm indicate the photocleavage of compound 1 into its products. (C) The modified MscL channel, which was reconstituted in synthetic lipids {1,2-dioleoyl-sn-glycero-3-phosphocholine, cholesterol, and 1,2-distearoyl-sn-glycero-3-phosphoethanolamine-N-[methoxy(polyethylene glycol)2000] in a molar ratio of 70:20:10, respectively} (25), was patched in the dark. Recordings were performed at +20 mV without a pressure gradient in a

bath and pipette buffer (200 mM KCl, 100 mM MgCl₂, 10 mM CaCl₂, 5 mM HEPES, pH = 6.5). Channel openings are shown as upward currents. The light from a high-pressure Hg lamp was directed toward the patch bath through a fiber optic cable, and the wavelength was adjusted by appropriate filters. Current did not flow in the dark even with applied pressure up to the magnitude at which the patch was lost. (D) The spontaneous channel openings in response to light were recorded in real time and with no applied pressure. There were no channel openings in the dark (before the triangle); however, upon exposure to light at $\lambda = 366$ nm (starting point indicated by a triangle), the channel opened spontaneously. (Inset) An expanded fragment of the trace marked by dashed lines.

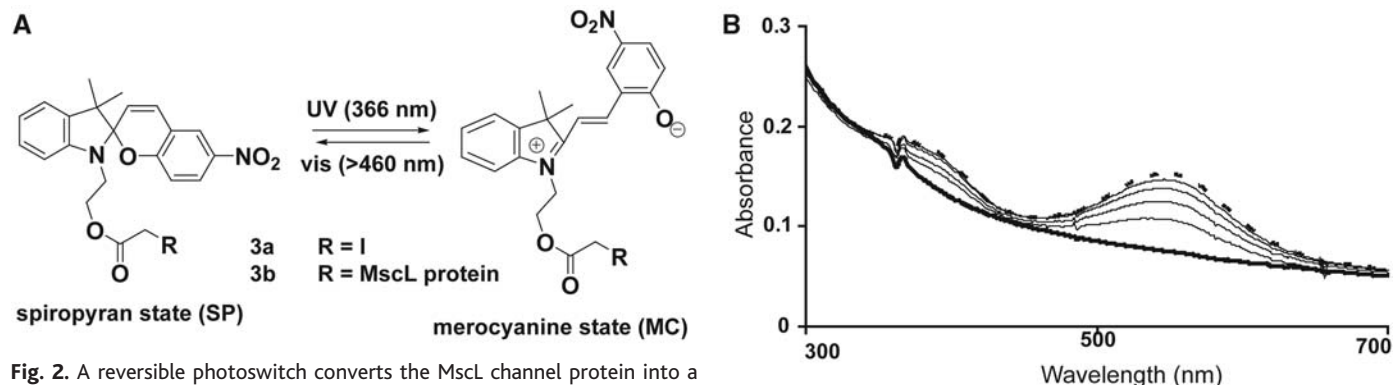
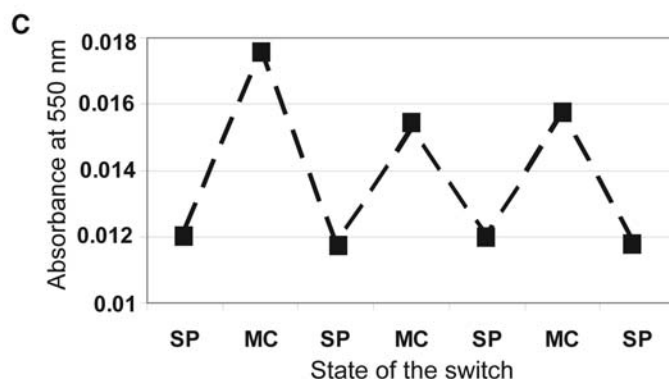


Fig. 2. A reversible photoswitch converts the MscL channel protein into a valve that can be opened and closed by optical signals. (A) Light-induced switching of compound 3. (B) UV-visible spectrum of 3b (MscL modified with compound 3a) in the SP form before irradiation with UV light (full thick line), in charged MC form after irradiation (dashed line), and at 20-s intervals during the irradiation process (full thin lines). (C) Switching cycles of MscL (3b) reconstituted in liposomes, followed by UV-visible spectroscopy at 550 nm under alternating irradiation with 366-nm UV light and >460-nm visible light (2 min each) (SP, spiropyran form and MC, merocyanine form).



ductance of the channel [see (24) for a detailed discussion].

We prepared several photosensitive compounds specifically to harness the hydration- and charge-mediated gating mechanism described above. In our design, illumination leads to a localized buildup of charge and consequent actuation of the valve. In the case of reversible operation, after initial actuation of the valve illumination with light of another wavelength neutralizes the localized charge and leads to valve closure.

In order to couple such photosensitive actuators specifically to the charge-sensitive part of the channel, we replaced the glycine residue at the 22nd amino acid position in M1 helices by cysteine (16), an amino acid that is not present anywhere else in the MscL protein. Five binding

sites in each MscL protein were then available for the actuators. Compound **1a**, designed to irreversibly charge the hydrophobic pore of the channel after irradiation, is a cysteine-selective alkylating reagent composed of an iodoacetate bearing the photocleavable protecting group 6-nitroveratryl alcohol (Fig. 1A) (25). This compound is sensitive to long-wavelength ultraviolet (UV), a wavelength range that is compatible with most biomaterials (26). Illumination at $\lambda > 300$ nm results in photolysis of the protective group, as shown by UV-visible absorption spectroscopy (Fig. 1B), for both free **1a** and the MscL-bound form **1b**. The disappearance of the absorption band at 346 nm and the appearance of the band at 374 nm are typical for the cleavage of esters of 6-nitroveratryl alcohol, producing free acid

and 6-nitroveratryl aldehyde (27). UV photolysis of modified MscL **1b** leaves cysteine-bound acetates **2**, which are negatively charged above pH = 4.0, inside the channel.

The functionality of the resulting protein valve was assessed at the single-molecule level by measuring the ionic current flowing through this modified channel in patch clamp experiments. The modified MscL was reconstituted in synthetic lipids, and patch clamp studies were performed in the presence and absence of UV light in the excised inside-out patch configuration; that is, the inner leaflet of the bilayer formerly facing the liposomal interior becomes exposed to the bath solution. No current flows through the channel in the dark, even if negative pressure is applied up to the breaking point of the patch (Fig. 1C). However, when the proteoliposomes are exposed to UV light, the channel opens even in the absence of applied pressure (Fig. 1D) (28).

Having achieved the conversion of the channel protein into a molecular valve actuated by light, we set out to incorporate controlled reversibility. To this end, a photoinduced switch, **3a**, based on a spiropyran core attached to a cysteine-selective iodoacetate moiety was synthesized and coupled to MscL to give **3b** (Fig. 2A). Upon irradiation at 366 nm, photochemical ring opening takes place, resulting in a charged zwitterionic merocyanine structure (MC) as indicated by the appearance of the new absorption maxima at 392 and 552 nm (Fig. 2B). Exposure to visible light (>460 nm) results in the reverse, ring-closing reaction, restoring the original uncharged spiropyran state (SP). This switching cycle can be repeated many times without a noticeable loss of photoactivity of the switch in buffer solution. However, when the switch was attached to the protein, the amount of merocyanine formed on irradiation consistently dropped after the first open-close cycle (Fig. 2C). Because the polarity of the local environment influences the photoequilibrium between the isomers, this result implies a permanent change within the protein after the first UV-visible cycle.

We induced reversible switching between open and closed states of the resulting modified photoactive protein **3b** embedded in a lipid membrane in patch clamp experiments (Fig.

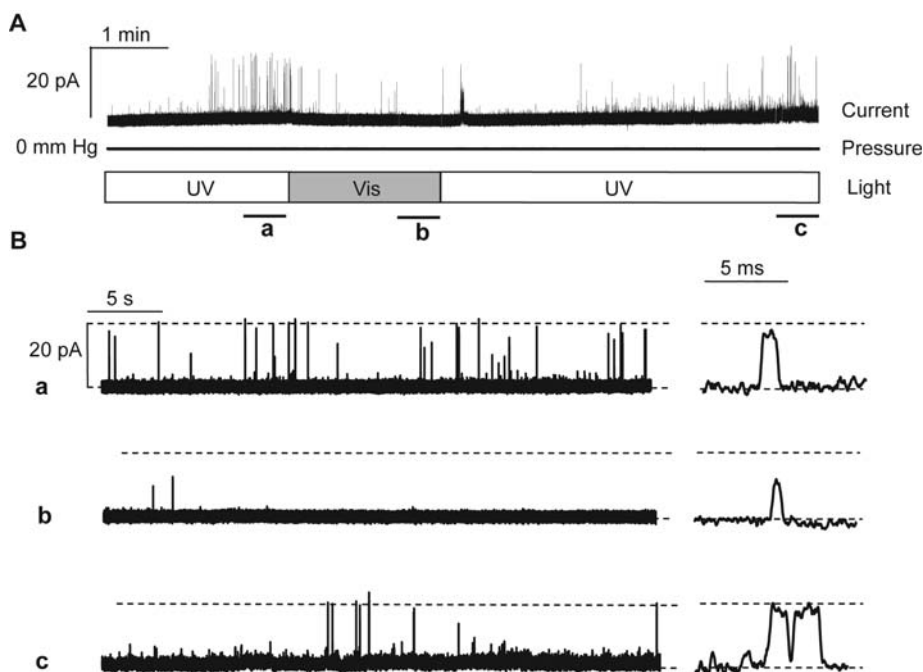
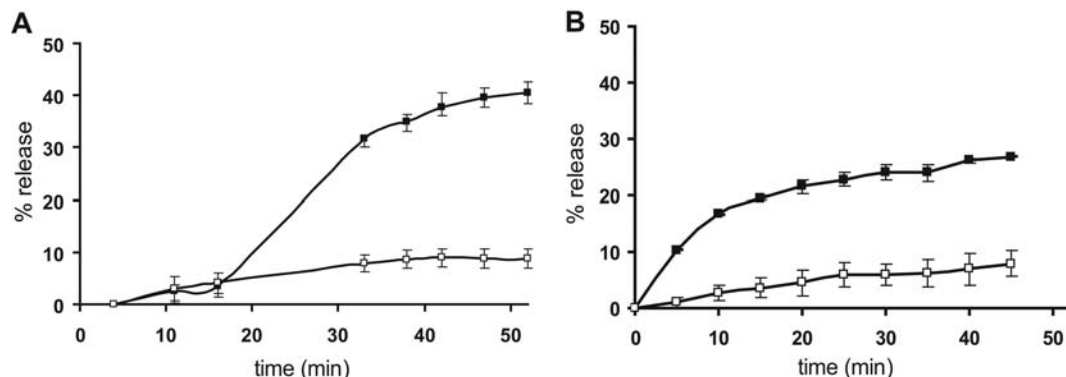


Fig. 3. Electrophysiological analysis of reversible functioning of modified MscL. (A) Single-channel recordings were performed at +20 mV without a pressure gradient, and channel openings are shown as upward currents. The patch was sequentially illuminated with UV and visible light by alternating the filter in the light source. Exposure wavelength is indicated under the patch trace. (B) Enlarged view of the channel openings at the end of each stimulation. The letters correspond to the positions indicated in the upper trace; (a) and (c) indicate the channel opened by UV, and (b) indicates channel closed by visible light. The first channel of each trace is shown on the right on a magnified time scale.

Fig. 4. Functioning of the light-actuated MscL in proteoliposomes. (A) Unidirectional operation of modified MscL **1b**. The release of liposomal content was calculated from the relative increase in fluorescence. Open squares indicate the calcein release in the dark, and solid squares indicate MscL-mediated release upon irradiation at 366 nm. (B) Reversible operation of modified MscL **3b**. Open squares indicate the fluid release in the dark, and solid squares indicate continuous light-actuated MscL-mediated release. Bars indicate the experimental error of the measured fluorescence to one standard deviation.



3A). In 23 recordings of individual samples from five separate membrane preparations, channel gating started within 2 min of irradiation at 366 nm in the absence of applied tension. The channel opened during this “on” state with a conductance of 0.5 to 1 nS, which increased to 1.5 nS after application of a pressure gradient [Supporting Online Material (SOM) Text]. UV-induced openings of the channels consistently start after a lag period. This delay in activation is consistent with a comparable 2-min time scale observed in the absorption spectra for the neutral-to-zwitterionic isomerization to reach completion (Fig. 2B). Once activated, however, the channels continue to work. If the patch is then irradiated with visible light, the channel activity drops substantially within seconds and the channels switch off. The rapid deactivation, contrasted with the slow activation, suggests a critical polarity (dependent on the number of switches in the zwitterionic MC form) necessary for ion conduction through the hydrophobic pore of the homopentamer channel. It is not yet clear how many charges are necessary to open the pore.

Irradiation of the closed channel with a second UV cycle follows the same pattern as in the first cycle, and, after a lag period, channel openings are evident from current flow. Figure 3B shows representative channel activity during the last 40 s of each irradiation period. There are many channel opening events during the first UV period, whereas there are no channel openings at the end of the visible light treatment. The lower number of channel openings on the second UV treatment compared with the first correlates with the lower amount of the zwitterionic MC form seen in the absorption spectrum (Fig. 2C) after the first cycle of illumination.

In order to test the utility of the light-addressable nanovalve in controlling the exchange of solutes other than ions across a membrane, we conducted classical efflux experiments with a liposomal system containing a self-quenching fluorescent dye, calcein. The use of such calcein-loaded liposomes to monitor the permeability of liposomal membranes is a long-standing practice in the field of liposomal drug delivery (29). Because of the high local concentration inside the liposomes, the fluorescence intensity of calcein is low, but release from these liposomes results in dilution of the dye and consequently a large increase in fluorescence signal. Here, we adapted this method to study the gating of MscL under isosmotic conditions. We reconstituted the modified photoactive MscL into liposomes and analyzed the response of the fluorescence signal to activation of the channel. In the case of the unidirectional nanovalve **1b**, some slow dye leakage (10%) was observed under ambient conditions without specific light stimulation, but 366-nm irradiation resulted in 43% release of liposomal content on the same time scale (Fig. 4A). As expected, proteoliposomes containing unmodified MscL did not release dye irrespective of illumination, nor did liposomes without protein.

Similar light-induced release of calcein under isosmotic conditions was observed for the reversible nanovalve (Fig. 4B). In this case, however, the amount released was lower compared with the one-way switch even though the reconstitution conditions were the same. The major difference between the two photosensitive molecules is their hydrophobicity, which is a key parameter for inducing spontaneous gating of this otherwise mechanosensitive channel. The calculated hydrophobicity of the reversible switch is higher than that of the one-way switch. These results are nonetheless a clear step toward a practical, photogated nanoscale delivery system.

References and Notes

- B. L. Feringa, *Molecular Switches* (Wiley, New York, 2001).
- K. Ichimura, S.-K. Oh, M. Nakagawa, *Science* **288**, 1624 (2000).
- C. Bertarelli, A. Bianco, F. D'Amore, M. C. Gallazzi, G. Zerbi, *Adv. Funct. Mater.* **14**, 357 (2004).
- J. H. Folgering, J. M. Kuiper, A. H. de Vries, J. B. Engberts, B. Poolman, *Langmuir* **20**, 6985 (2004).
- M. V. Alfimov, O. A. Fedorova, S. P. Gromov, *J. Photochem. Photobiol. A* **158**, 183 (2003).
- I. Willner, S. Rubin, *Angew. Chem. Int. Ed.* **35**, 367 (1996).
- S. Sukharev, A. Anishkin, *Trends Neurosci.* **27**, 345 (2004).
- N. Levina *et al.*, *EMBO J.* **18**, 1730 (1999).
- C. C. Cruickshank, R. F. Minchin, A. C. Le Dain, B. Martinac, *Biophys. J.* **73**, 1925 (1997).
- B. Ajouz, C. Berrier, A. Garrigues, M. Besnard, A. Ghazi, *J. Biol. Chem.* **273**, 26670 (1998).
- C. Berrier, A. Garrigues, G. Richarme, A. Ghazi, *J. Bacteriol.* **182**, 248 (2000).
- P. Blount, S. I. Sukharev, M. J. Schroeder, S. K. Nagle, C. Kung, *Proc. Natl. Acad. Sci. U.S.A.* **93**, 11652 (1996).
- C. C. Hase, A. C. Le Dain, B. Martinac, *J. Membr. Biol.* **157**, 17 (1997).
- P. Blount, M. J. Schroeder, C. Kung, *J. Biol. Chem.* **272**, 32150 (1997).
- X. Ou, P. Blount, R. J. Hoffman, C. Kung, *Proc. Natl. Acad. Sci. U.S.A.* **95**, 11471 (1998).
- K. Yoshimura, A. Batiza, M. Schroeder, P. Blount, C. Kung, *Biophys. J.* **77**, 1960 (1999).

- E. Perozo, A. Kloda, D. M. Cortes, B. Martinac, *J. Gen. Physiol.* **118**, 193 (2001).
- G. Chang, R. H. Spencer, A. T. Lee, M. T. Barclay, D. C. Rees, *Science* **282**, 2220 (1998).
- S. Sukharev, M. Betanzos, C. S. Chiang, H. R. Guy, *Nature* **409**, 720 (2001).
- E. Perozo, D. M. Cortes, P. Sompornpisut, A. Kloda, B. Martinac, *Nature* **418**, 942 (2002).
- J. Gullingsrud, K. Schulten, *Biophys. J.* **85**, 2087 (2003).
- K. Yoshimura, A. Batiza, C. Kung, *Biophys. J.* **80**, 2198 (2001).
- M. Sukhareva, D. H. Hackos, K. J. Swartz, *J. Gen. Physiol.* **122**, 541 (2003).
- A. Anishkin, C. S. Chiang, S. Sukharev, *J. Gen. Physiol.* **125**, 155 (2005).
- Materials and methods are available as supporting material on Science Online.
- C. G. Bochet, *J. Chem. Soc. Perkin Trans. 1* 125 (2002).
- R. Reinhard, B. F. Schmidt, *J. Org. Chem.* **63**, 2434 (1998).
- The hydrophilicity of the 22nd position of MscL determines the magnitude of tension required for channel opening (16). When glycine is replaced by cysteine, the higher hydrophobicity of cysteine stabilizes the closed state, and actuation requires a tension high enough to rupture the patch. The nitrophenyl derivative in modified MscL **1b** increases hydrophobicity even further. Therefore, we expect the channel not to open in the dark even if tension is applied up to the breaking point of the patch. However, upon illumination, the generation of charge at the same position leads to spontaneous opening in the absence of applied tension.
- R. R. C. New, *Liposomes: A Practical Approach* (IRL Press, Oxford, 1990), pp. 105–161.
- We thank the MscL team in Groningen for their contribution, B. Poolman and D. Stavenga for critical reading of the manuscript, the neurobiophysics group in University of Groningen for making available the patch clamp facilities, and the Netherlands Organization for Scientific Research (NWO-CW) (B.L.F.) and the Materials Science Centre (MSC plus), University of Groningen (M.W. and B.L.F.), for financial support.

Supporting Online Material

www.sciencemag.org/cgi/content/full/309/5735/755/DC1

Materials and Methods

SOM Text

Figs. S1 to S7

References and Notes

12 May 2005; accepted 14 June 2005
10.1126/science.1114760

Permanent El Niño–Like Conditions During the Pliocene Warm Period

Michael W. Wara, Ana Christina Ravelo,* Margaret L. Delaney

During the warm early Pliocene (~4.5 to 3.0 million years ago), the most recent interval with a climate warmer than today, the eastern Pacific thermocline was deep and the average west-to-east sea surface temperature difference across the equatorial Pacific was only $1.5 \pm 0.9^\circ\text{C}$, much like it is during a modern El Niño event. Thus, the modern strong sea surface temperature gradient across the equatorial Pacific is not a stable and permanent feature. Sustained El Niño–like conditions, including relatively weak zonal atmospheric (Walker) circulation, could be a consequence of, and play an important role in determining, global warmth.

The low-latitude Pacific Ocean provides a substantial portion of the global atmosphere's sensible and latent heat and is thus a central driver of climate (1). Over the past 25 years, the mean equatorial Pacific sea surface tem-

perature (SST) has increased by $\sim 0.8^\circ\text{C}$ (2), possibly in response to increasing greenhouse gas concentration (3). Changes in the tropical Pacific mean climatic state may influence the amplitude of interannual, or El Niño–Southern